First principles modeling of oxygen vacancy formation and mobility in (Ba,Sr)(Co,Fe)$O_{3-\delta}$ perovskites

R. Merkle[a], E.A. Kotomin[a,b], Y.A. Mastrikov[b,c], M.M. Kuklja[c], J. Maier[a]

[a]MPI Solid State Research Stuttgart, [b]Inst. Solid State Physics Riga, [c]University of Maryland

MPI for Solid State Research Stuttgart

$Ba_{1-x}Sr_xCo_yFe_{1-y}O_{3-\delta}$ perovskites: high concentration and mobility of $V_o^{\cdot\cdot}$

BSCF permeation membranes

⇔ high *D* (Z.P. Shao (2000))

test as SOFC cathode

⇔ high *k* (Z.P. Shao, S.M. Haile (2004))

mechanistic interpretation:

L. Wang, R. Merkle, J. Maier
J. Electrochem. Soc. 157 (2010) B1802

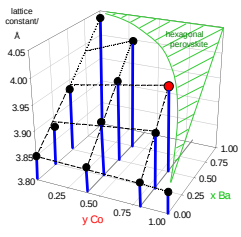

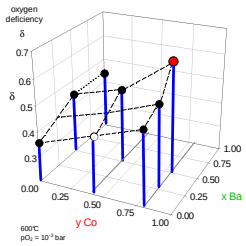

$D_{V_O^{\cdot\cdot}}$ from ^{18}O isotope exchange:

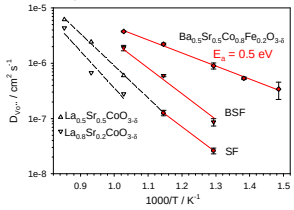

L. Wang et al., *Appl. Phys. Lett.* 94 (2009) 071908
LSC: R.A. De Souza et al.,*Solid State Ionics* 106 (1998) 175

Computational details

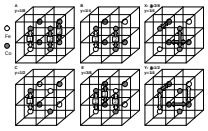

different vacancy configurations in supercell

* VASP 4.6 + PAW and plane wave basis set
* PBE-type exchange-correlation GGA functional
* 4x4x4 k-point mesh in the Brillouin zone (Monkhorst-Pack scheme)
* ion charges calculated by the Bader method
* energy cut-off 520 eV
* $Ba_4Sr_4(Co,Fe)_4O_{12-\delta}$ supercells (2×2×2)
* Fe: high spin state, Co: intermediate spin

E. A. Kotomin et al., Solid State Ionics 188 (2011) 1

Electronic structure

spin-projected density of states (DOS) for $Ba_{0.5}Sr_{0.5}Co_{0.75}Fe_{0.25}O_{2.875}$

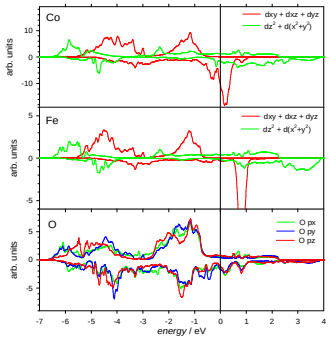

cartoon of the BSCF band structure (density of states)

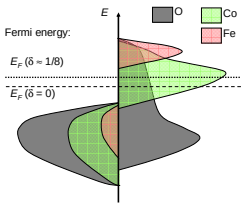

significant (Fe,Co)-O covalency (t_{2g})
Fe: 1 eV gap between occupied ↑ e_g and empty ↓ e_g

oxygen loss for δ = 1/8: excess electrons distributed mainly to Co and O

cf. XAS study for $Ba_{0.1}Sr_{0.9}Co_{0.8}Fe_{0.2}O_{3-\delta}$:
charge distribution depends delicately on δ (more e to Fe at low *T*, high pO_2)

D.N. Mueller et al., *J. Mat. Chem.* 19 (2009) 1960

Oxygen vacancy formation

$O_O^x + 2\,M_M^x \rightleftharpoons 0.5\,O_2 + V_O^{\cdot\cdot} + 2\,M_M'$

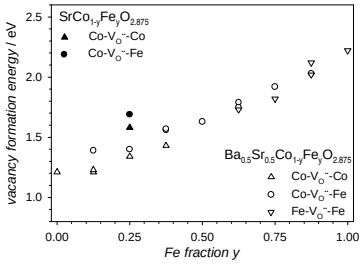

BSCF ≃ linear increase of $V_O^{\cdot\cdot}$ formation energy with Fe content
⇔ more narrow empty Fe states at higher energy

SCF: slightly higher values
⇔ oversized Ba favours reduction of Fe,Co

comparison to expt. data:
E_V = 0.6 eV for BSF (δ = 0.34),
0.5 eV for BSCF (δ = 0.52)

L. Wang et al., *ECS Transact,* 13(26) (2008) 85

E_V depends on δ ⇒ extrapolate to δ = 1/8
trend of smaller E_V for Co-rich materials confirmed

Oxygen vacancy migration

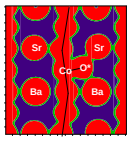

transition state:
e density map in (110) plane
for $Ba_{0.5}Sr_{0.5}Co_{0.75}Fe_{0.25}O_{2.875}$

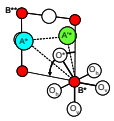

transition state:
O* moving through "critical triangle"

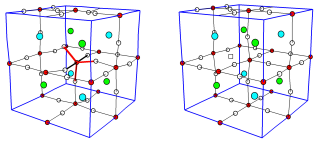

transition state and initial state
for $Ba_{0.5}Sr_{0.5}CoO_{2.875}$

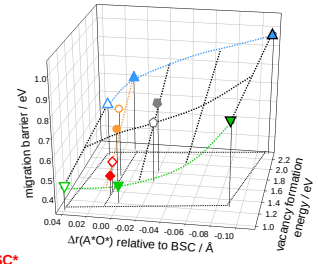

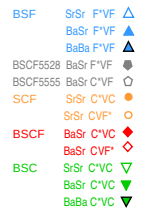

geometric factors:
d_{A-O^*} compared to BSC*
(cf. SrSr, SrBa and BaBa barriers for BSC)

electronic factors:
vacancy formation energy
(cf. SrBa barriers for BSC, SCF, BSF)

barriers	DFT	expt.	good
BSCF	0.44 eV	0.5 eV*	agreement
BSF	0.72 eV	1.0 eV*	
SCF	0.64 eV	0.65 eV**	

*L. Wang et al., *JES* 157 (2010) B1802
**Y. Teraoka et al., *Mat. Res. Bull.* 23 (1988) 51

Vacancy formation energy E_v, migration barrier E_m, and structural parameters of oxygen migration.
* indicates the migrating O and directly connected cations. Italic numbers give the change in the transition state relative to the ideal structure. Δq(O*) is the change of O* ion charge in the transition state relative to the initial state. For BSCF and SCF, the geometry and barrier from a Co-$V_O^{\cdot\cdot}$-Co initial state to a Co-$V_O^{\cdot\cdot}$-Co final state as well as for Fe-$V_O^{\cdot\cdot}$-Co to Fe-$V_O^{\cdot\cdot}$-Co (Fe*-O* transition state) is given

E_V / eV	E_m / eV	B*-O* / Å	B*-O_v / Å	B*-O_h / Å	q(O*) Δq(O*) / e_0	B*-B** / Å	A*-O* Sr / Å	A*-O* Ba / Å	A*A'* / Å
BSC	BaSr	1.70	1.77	1.95	-0.97	5.68	2.37	2.58	4.12
1.21	**0.40**	*-13%*	*-9%*	*±0%*	*+0.10*	*+3%*			*+6%*
	SrSr	1.71	1.79	1.95	-0.96	5.48	2.41		4.19
1.03	**0.43**	*-12%*	*-8%*	*±0%*	*+0.11*	*-1%*			*+7%*
	BaBa	1.68	1.76	1.95	-0.95	5.63		2.49	4.12
1.28	**0.75**	*-14%*	*-10%*	*±0%*	*+0.12*	*+2%*			*+6%*
BSCF	BaSr								
1.34	**0.42**	1.69	1.77	1.98	-0.98	5.75	2.38	2.59	4.10
C*VC->C*VC		*-13%*	*-9%*	*+1.5%*	*+0.09*	*+4%*			*+5%*
1.40	**0.46**	1.69	1.76	1.91	-0.95	5.65	2.39	2.57	4.15
CVF*->CVF*		*-13%*	*-10%*	*-2%*	*+0.13*	*+2%*			*+6%*
BSF	BaSr	1.68	1.78	1.95	-0.96	5.68	2.40	2.57	4.14
2.22	**0.72**	*-14%*	*-9%*	*±0%*	*+0.12*	*+3%*			*+6%*
SCF	SrSr								
1.58	**0.60**	1.70	1.79	1.92	-0.97	5.56	2.38		4.08
C*VC->C*VC		*-11%*	*-7%*	*±0%*		*+2%*			*+6%*
1.69	**0.67**	1.70	1.77	1.91	-0.97	5.52	2.38		4.11
CVF*->CVF*		*-11%*	*-8%*	*-2%*		*+2%*			*+7%*

E.A. Kotomin, R. Merkle, Y. A. Mastrikov, M. M. Kuklja, J. Maier, *ECS Transact.* 35(1) (2011) 823; *JES* (2011) submitted

Summary

*** vacancy formation energy increases linearly with Fe content**
↔ difference in band structure

*** vacancy migration barriers in good agreement with experiments**

*** barriers are determined by combination of**
geometrical constraints ($d_{A^*-O^*}$ in transition state)
***and* electronic contribution (vacancy formation energy)**

Acknowledgement

The research leading to these results has received funding from the European Union's Seventh Framework Program FP7/2007-2013 (NASA-OTM) under grant agreement n°228701 and the US National Science Foundation (NSF) grant n°08 32958. Authors thank NSF for its support through TeraGrid resources provided by the Texas Advanced Computing Center (TACC) and the National Center for Supercomputing Applications (NCSA) under grant number TG-DMR100021. MMK is grateful to the Office of the Director of NSF for support under the IRD Program. Any appearance of findings, conclusions, or recommendations, expressed in this material are those of the authors and do not necessarily reflect the views of NSF. This study was supported also by a grant of computer time at the EMS Laboratory at PNNL (Project No 42498).
Authors are greatly indebted to D. Gryaznov for many stimulating discussions.